



ORIGINAL ARTICLE

Prenylated sulfonyl amides from the leaves of *Glycosmis pentaphylla* and their potential anti-proliferative and anti-inflammatory activities



Wenli Xie ^{a,1}, Hefeng Nian ^{b,1}, Xueni Li ^a, Jing Xu ^a, Yu Chen ^b, Zhinan Mei ^{c,*}, Guangzhong Yang ^{a,*}

^a School of Pharmaceutical Sciences, South-Central Minzu University, Wuhan 430074, PR China

^b College of Chemistry and Material Sciences, South-Central Minzu University, Wuhan 430074, PR China

^c College of Plant Science & Technology, Huazhong Agricultural University, Wuhan 430072, PR China

Received 28 August 2022; accepted 12 December 2022

Available online 16 December 2022

KEYWORDS

Glycosmis pentaphylla;
Rutaceae;
Sulphur-containing amides;
Anti-inflammatory activity;
Anti-proliferative activity

Abstract Six previously undescribed sulfur-containing amides were isolated from the leaves of *Glycosmis pentaphylla*. Their structures were delineated by HRESIMS, 1D and 2D NMR, electronic circular dichroism (ECD) calculations, and DP4+ analyses based on gauge-independent atomic orbital (GIAO) NMR calculations. Compounds 1–4 belong to the type of methylsulfonylpropenoic acid amides. Through different cyclization pathways of geranyloxy, compounds 1 and 2 carry uncommon cyclohexane-1, 3-diol and cyclohex-3-en-1-ol moiety, respectively. Compound 3 is the oxidation product of the double bond $\Delta^{6''(7'')}$ of geranyloxy. Compound 5 is elucidated as the type of methylsulfonylpropanoic acid amide. Compound 6 represents a rare sulfur-containing amide possessing a morpholin-3-one moiety. All isolated compounds were evaluated for their anti-inflammatory and anti-proliferative activities. Compound 4 significantly inhibited lipopolysaccharide-induced nitric oxide (NO) production in mouse macrophage RAW 264.7 cells with the IC₅₀ value of 0.55 μ M. Moreover, compounds 3 and 4 exhibited different anti-proliferative activities against HepG-2 with IC₅₀ values of 11.52 and 9.41 μ M, respectively.

© 2022 The Author(s). Published by Elsevier B.V. on behalf of King Saud University. This is an open access article under the CC BY-NC-ND license (<http://creativecommons.org/licenses/by-nc-nd/4.0/>).

1. Introduction

The genus *Glycosmis* belongs to the Rutaceae family, and many secondary metabolites with pharmacological and biological activities, such as alkaloids, flavonoids, and phenolic glycosides, are isolated from various parts of the *Glycosmis* plant (Yasir et al., 2019). Sulfur-containing amides are a special type of alkaloids, mainly derived from plants such as *Glycosmis*, and fungi, which are classified into four types (Hofer and Greger, 2000), including methylthiopropionic acid amides, methylsulfinylpropenoic acid amides, methylsulfonylpropenoic acid

* Corresponding authors.

E-mail addresses: meizhinan@mail.hzau.edu.cn (Z. Mei), yangguangzhong@mail.scuec.edu.cn (G. Yang).

¹ These authors contributed equally to this work.

Peer review under responsibility of King Saud University.



Production and hosting by Elsevier

amides (MSPAAs), and methylthiocarbonic acid amides (Sutton et al., 1994). The structural characteristics of MSPAAs have a prenyloxy or geranyloxy in the *para* position of the benzene ring of the phenethylamide moiety. The structural diversity mainly comes from the oxidation of the geranyloxy side chain to form oxidation products such as hydroxyl, aldehyde, and ketone derivatives, or intramolecular cyclization to form dihydrofuranone rings containing ether and ketone functional groups (Yang et al., 2015; Greger et al., 1994; Hofer et al., 1995; Hofer et al., 2000; Hofer et al., 1998; Vajrodaya et al., 1998). Owing to their unique structure and biological activity, MSPAAs have attracted the attention of synthetic organic chemists, and the total synthesis of methylgerambullone has been completed (Moon et al., 2010).

Glycosmis pentaphylla (Retz.) DC. is an evergreen shrub native to tropical and subtropical regions of China, India, and other countries, and is used as traditional medicine to treat a variety of chronic diseases including cough, fever, inflammation, bronchitis, rheumatism, diabetes, cancer, and more (Khandokar et al., 2021). Previously, our research group performed phytochemical studies of *G. pentaphylla* leaves and isolated 18 previously undescribed sulphur-containing amides. Methylgerambullin has the strongest inhibitory effect on the proliferation of HepG2 cells, and its inhibitory effect on NO production is about 37 times that of the positive drug dexamethasone. Moreover, the antitumor mechanism of methylgerambullin is based on the activation of mitochondrial and endoplasmic reticulum stress signaling

pathways and inhibition of AKT and STAT3 pathways (Nian et al., 2020; Wu et al., 2021). Taken together, these findings prompted us to isolate more sulphur-containing amides from *G. pentaphylla* leaves and evaluate their biological activities. Thus, six previously undescribed sulphur-containing amides were separated from the leaves of *G. pentaphylla* (Fig. 1). In addition, all isolated compounds were evaluated for their anti-inflammatory and anti-proliferative properties.

2. Materials and methods

2.1. General experimental procedures

Optical rotation in MeOH was determined using an Autopol IV polarimeter (Rudolph Research Analytical, Hackettstown, NJ, USA). UV spectra were obtained using a UH5300 UV–vis Double Beam spectrophotometer (Hitachi Co., Tokyo, Japan). 1D and 2D NMR spectra were recorded with CD₃OD on a Bruker AVANCE III™ 600 M Hz spectrometer (Bruker, Ettlingen, Germany) using tetramethylsilane (TMS) as the internal standard. Chemical shifts (δ) are expressed in ppm and coupling constants (J) are expressed in Hz. HR-ESI-MS data were acquired using a Thermo Scientific Q Exactive Orbi-

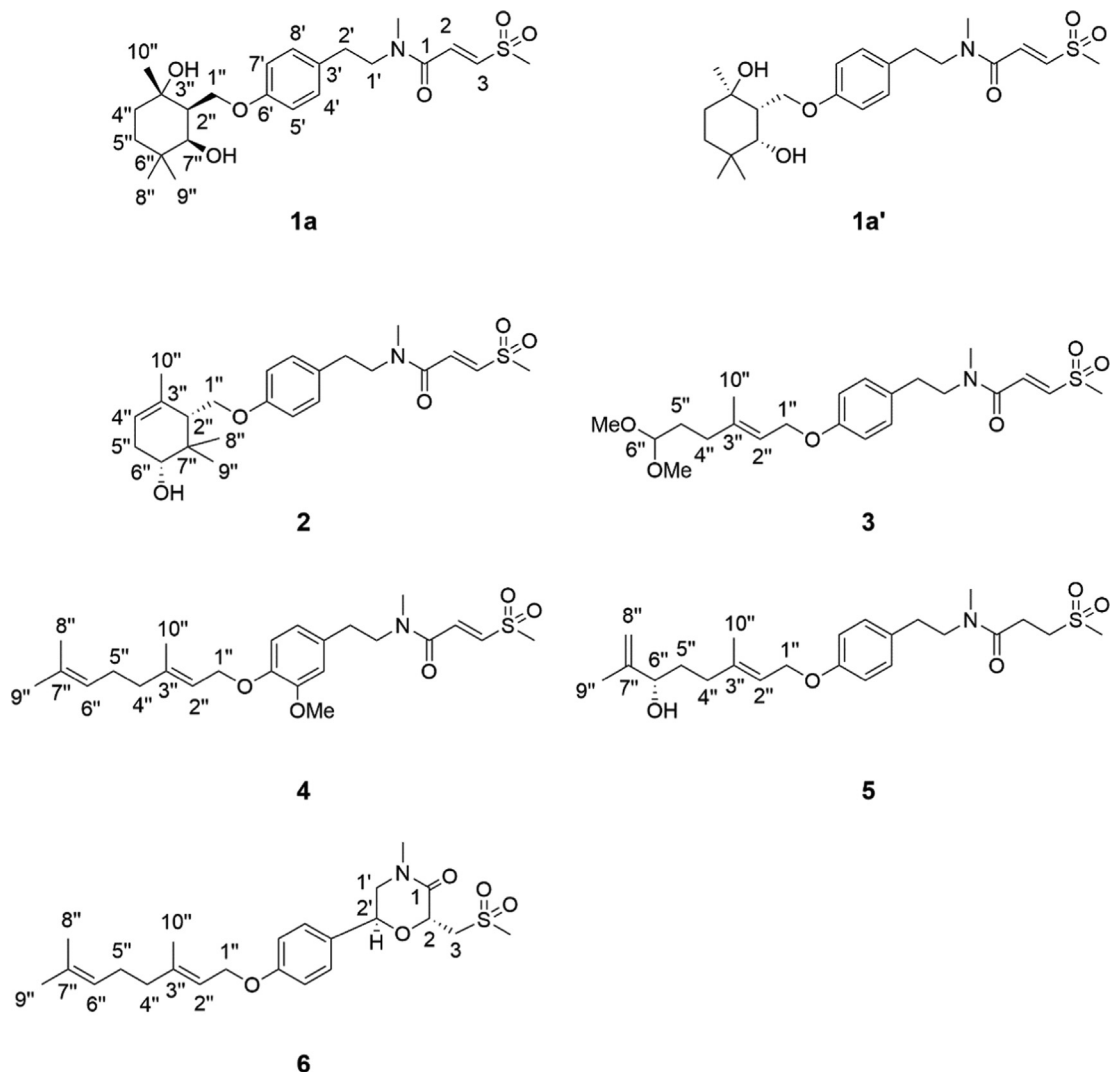


Fig. 1 Structures of compounds 1–6.

trap LC-MS/MS System (Thermo Scientific, Waltham, MA, USA). The preparation of compounds were performed on an Ultimate 3000 HPLC system (Thermo Fisher Scientific Dionex., Sunnyvale, CA, USA) with an Ultimate 3000 pump and an Ultimate 3000 Variable Wavelength detector. The HPLC conditions were described as follows: column: Nacalai Tesque 5C₁₈-MS-II (250 × 10 mm, 5 μm), flow rate: 3 ml/min, detection wavelengths: UV, 220 and 254 nm. Silica gel for CC (200–300 mesh and 300–400 mesh) was obtained from the Qingdao HaiYang Chemical Group Co. Ltd. (Qingdao, China). Chromatographic grade acetonitrile and methanol were purchased from Chang Tech Enterprise Co. Ltd. (Taiwan, China). The human tumor cell line HepG2 and RAW264.7 murine macrophages were purchased from the cell bank of the Chinese Academy of Sciences (Shanghai, China). Cisplatin was purchased from Sigma-Aldrich (Saint Louis, MO, USA). Dexamethasone and lipopolysaccharide (LPS) were purchased from Sigma Chemical Co. Ltd. (St. Louis, MO, USA). Cell Counting Kit (CCK-8) was purchased from Beyotime Biotechnology (Shanghai, China). The NO kit was purchased from Shanghai Biyuntian Biotechnology Co. Ltd. (Shanghai, China). Dulbecco's modified Eagle's medium (DMEM) and penicillin-streptomycin solution were purchased from GE Healthcare Life Sciences (Logan, UT, USA). Fetal bovine serum (FBS) was purchased from Gibco, Life Technologies (Grand Island, NY, USA). Reagent grade DMSO was purchased from Vetec, Sigma Chemical Co. Ltd. (St. Louis, MO, USA). Absorbance was recorded on a Multiskan GO microplate reader (Thermo Fisher Scientific, Inc., Waltham, MA, USA). The organic solvent was acquired from Sinopharm Chemical Reagent Co., Ltd. (Shanghai, China).

2.2. Plant material

The leaves of *G. pentaphylla* were collected from Mengyang Town, Jinghong City, Xishuangbanna Dai Autonomous Prefecture, Yunnan Province (north latitude 22°8'48"; east longitude 100°56'29"), and identified by Prof. Zhao Yinghong from Institute of Ethnic Medicine, Xishuangbanna Dai Autonomous Prefecture. The voucher specimen was deposited in the herbarium of the School of Pharmaceutical Sciences, South-Central Minzu University.

2.3. Extraction and isolation

12 kg of dried leaves of *G. pentaphylla* were powdered and extracted three times with 90 % EtOH at room temperature to obtain EtOH extract (860 g), which was then successively partitioned with petroleum ether (P.E.) and MeOH to acquire P.E. extract 100 g and MeOH extract 740 g. The MeOH extract (740 g) was subjected to polyamide column (80–100 mesh), and eluted with a gradient of EtOH-H₂O (0:1, 3: 7, 1: 1, 7: 3, 95: 5) to give 5 subfractions (Fr.1-Fr.5). Fr.1 (100.9 g) was purified by a silica gel column chromatography (CC) eluted with CH₂Cl₂-MeOH (100:1, 50:1, 20:1, 9:1, 5:1) to provide 12 subfractions (Fr.1.1-Fr.1.12). Fr.1.4 (4.9 g) was subjected to a silica gel CC eluted with P.E.-EtOAc (8:2, 6:4, 4:6, 0:1), and then separated by semi-preparative HPLC (MeOH-H₂O, 82:18, v/v) to yield compound **2** (1.1 mg, *t_R* = 6.4 min). Fr. 1.6 (8.0 g) was chromatographed on silica gel column by eluting with P.E.-EtOAc (8:2, 6:4, 4:6, 2:8),

and then further purified by semi-preparative HPLC (MeOH-H₂O, 60:40, v/v) to yield compounds **1** (8.1 mg, *t_R* = 12.2 min) which was further resolved by chiral column [column: CHIRALPAK® IC 4.6 × 250 mm 5 μm; mobile phase: MeCN: H₂O (30:70); flow rate: 0.5 ml/min; detection: UV, 225 nm] to give a pair of enantiomer **1a** and **1a'** at *t_R* 54.3 and 46.9 min respectively, and **5** (8.2 mg, *t_R* = 32.3 min). Fr. 2 (89.7 g) was subjected to a silica gel CC eluted with CH₂-Cl₂-MeOH (100:1, 20:1, 9:1, 8:2, 0:1) to obtain 13 fractions (Fr. 2.1-Fr.2.13). Fr. 2.5 (9.3 g) was subjected to ODS CC eluted with MeOH-H₂O (1:0, 7:3, 1:1, 3:7, 0:1) to obtain 7 fractions (Fr.2.5.1-Fr.2.5.7). Fr.2.5.4 (0.5 g) was further separated by a silica gel CC with a gradient of P.E.-EtOAc (9:1, 7:3, 4:6, 0:1), and then purified by semi-preparative HPLC (MeCN-H₂O, 70:30, v/v) to give compound **4** (2.0 mg, *t_R* = 14.5 min). Fr.2.6 (1.8 g) was subjected to silica gel CC by eluting with P. E.-EtOAc (8:2, 6:4, 2:8, 0:1), and then purified by semi-preparative HPLC (MeCN-H₂O, 60:40, v/v) to afford compound **6** (3.8 mg, *t_R* = 31.0 min). Fr.2.8 (31.6 g) was separated by a silica gel CC with a gradient of CH₂Cl₂-EtOAc (9:1, 7:3, 4:6, 0:1) to yield subfraction Fr.2.8.4 (6.9 g), which was further purified by a silica gel CC eluted with P.E.-EtOAc (8:2, 6:4, 4:6, 0:1) to obtain 10 subfractions (Fr.2.8.4.1-Fr.2.8.4.10). Fr.2.8.4.10 (2.95 g) was further purified by a silica gel CC eluted with P.E.-CH₂Cl₂ (1:0, 7:3, 3:7, 0:1) and CH₂Cl₂-MeOH (50:1, 9:1, 0:1), and then purified by semi-preparative HPLC (MeCN-H₂O, 51:49, v/v) to give compound **3** (4.0 mg, *t_R* = 15.1 min).

Spectroscopic Data

Glycopentamide S (**1**): colorless oil; UV (MeOH) λ^{max} (log ε) 225 (4.05), 270 (3.60); ¹H NMR data see Table 1 and ¹³C NMR data see Table 3; HRESIMS *m/z* 476.20764 [M + Na]⁺ (calcd for C₂₃H₃₅NO₆SNa, 476.20773).

Glycopentamide S (**1a**): [α]_D²⁰ +0.049 (MeOH, *c* = 0.05); ECD (1.05 × 10⁻⁴ M, MeOH) λ(θ) 206 (-0.25), 229 (+2.29), 242 (+0.09), 275 (+1.13) nm;

Glycopentamide S (**1a'**): [α]_D²⁰ -0.051 (MeOH, *c* = 0.05); ECD (1.05 × 10⁻⁴ M, MeOH) λ(θ) 212 (+0.06), 228 (-2.09), 245 (-0.11), 277 (-1.01) nm;

Glycopentamide T (**2**): colorless oil; [α]_D²⁰ +49.26 (MeOH, *c* = 0.05); UV (MeOH) λ^{max} (log ε) 225(3.97), 270 (3.44); ECD (6.55 × 10⁻⁵ M, MeOH) λ(θ) 200 (+16.20), 209 (-0.96), 223 (+3.79) nm; ¹H NMR data see Table 1 and ¹³C NMR data see Table 3; HRESIMS *m/z* 458.19687 [M + Na]⁺ (calcd for C₂₃H₃₃NO₅SNa, 458.19716).

Glycopentamide U (**3**): colorless oil; UV (MeOH) λ^{max} (log ε) 230 (4.21), 270 (4.02); ¹H NMR data see Table 1 and ¹³C NMR data see Table 3; HRESIMS *m/z* 462.19199 [M + Na]⁺ (calcd for C₂₂H₃₃NO₆SNa, 462.19208).

Glycopentamide V (**4**): colorless oil; UV (MeOH) λ^{max} (log ε) 235 (3.89), 275 (3.83); ¹H NMR data see Table 2 and ¹³C NMR data see Table 3; HRESIMS *m/z* 450.23120 [M + H]⁺ (calcd for C₂₄H₃₆NO₅S, 450.23087).

Glycopentamide W (**5**): colorless oil; [α]_D²⁰ +7.78 (MeOH, *c* = 0.05); UV (MeOH) λ^{max} (log ε) 225(4.06), 275 (3.24); ECD (1.09 × 10⁻⁴ M, MeOH) λ(θ) 231 (+0.71), 260 (-0.07), 275 (+0.18) nm; ¹H NMR data see Table 2 and ¹³C NMR data see Table 3; HRESIMS *m/z* 460.21243 [M + Na]⁺ (calcd for C₂₃H₃₅NO₅SNa, 460.21282).

Glycopentamide X (**6**): colorless oil; [α]_D²⁰ +566.7 (MeOH, *c* = 0.01); UV (MeOH) λ^{max} (log ε) 205 (4.35), 225 (4.19),

275 (3.30); ECD (2.18×10^{-5} M, MeOH) $\lambda(\theta)$ 200 (+2.43), 208 (-0.76), 217 (+0.90), 231 (-2.11) nm; ^1H NMR data see Table 2 and ^{13}C NMR data see Table 3; HRESIMS m/z 458.19693 $[\text{M} + \text{Na}]^+$ (calcd for $\text{C}_{23}\text{H}_{33}\text{NO}_5\text{SNa}$, 458.19716).

2.4. NMR calculations

Computational NMR data were obtained from the IEFPCM model at the mPW1PW91/6-311 + G(2d,p) level in methanol using the GIAO (gauge-independent atomic orbital) method. (Detailed NMR calculations are provided in Supplementary Information).

2.5. ECD calculations

The ECD in methanol was calculated using the IEFPCM model with time-dependent density functional theory (TD-DFT). (See Supplementary Information for detailed ECD calculations).

2.6. Anti-proliferative activity bioassay

The anti-proliferative activity of the isolated compounds on HepG-2 cell line was measured by the CCK-8 method according to the previously described protocol (Chen et al., 2019). In short, 5×10^3 HepG2 cell lines per well (in 100 μL of culture medium) were seeded in 96-well plates. After being treated with gradient concentrations (20 μM , 10 μM , 5 μM , 2.5 μM and 1.25 μM) of each compound at 37 $^\circ\text{C}$ for 24 h, the supernatant was discarded. Then, 100 μL cell culture medium containing 10 % CCK-8 solution was added to each well at 37 $^\circ\text{C}$ for 1 h. The absorbance values of each well at 450 nm were measured on a microplate spectrophotometer. Cisplatin was used as the positive control.

2.7. Anti-inflammatory activity bioassay

The cell viability was firstly determined by the CCK-8 method. RAW264.7 cells were seeded into 96-well plates (2×10^5 cells per well) and cultured overnight. After treated with LPS (1.0 $\mu\text{g}/\text{mL}$) for 24 h, the culture medium was replaced by new medium containing gradient concentrations of each compound (20 μM , 10 μM , 5 μM , 2.5 μM and 1.25 μM). Dexamethasone was used as the positive control. After 24 h incubation, the supernatant was collected to determine NO content using Griess reagent. (Teng et al., 2019).

3. Results and discussion

All isolated compounds are obtained as colorless oils and belong to the sulphur-containing amides through HR-ESI-MS data, which are the characteristic components of this plant. Moreover, two sets of resonance signals are observed in the ^1H and ^{13}C spectrum of compounds 1–5 (Tables 1–3), indicating that these compounds are composed of two inseparable conformers. A comparison of NMR data of 1–4 with those of methylumbelliferone indicates that compounds 1–4 contain (*E*)-3-(methylsulfonyl)propenoic acid moiety and *N*-methyltyramine part. The rotation of the C–N amide bond is restricted due to the presence of the *N*-methyl group, resulting in two conformers, (a) *s-cis* and (b) *s-trans*, in which the ratio of the two conformers a/b ranges from 50 % to 75 % by ^1H NMR spectrum analysis. To facilitate structural analysis, we describe the structural identification of compounds 1–5 based on NMR data of conformer (a) (Greger et al., 1994).

The molecular formula of 1 was deduced to be $\text{C}_{23}\text{H}_{35}\text{NO}_6\text{S}$ through HR-ESI-MS (Fig. S9, Supplementary Information abbreviated SI) at m/z 476.20764 $[\text{M} + \text{Na}]^+$ (calcd for $\text{C}_{23}\text{H}_{35}\text{NO}_6\text{SNa}$, 476.20773), which was composed of two con-

Table 1 ^1H Spectroscopic Data for Compounds 1–3 in CD_3OD .

No.	1 ^a	1 ^a	2 ^a	2 ^a	3 ^a	3 ^a
2	6.83 (d, 15.0)	7.34 (d, 15.0)	6.85 (d, 15.0)	7.34 (d, 15.0)	6.82 (d, 15.0)	7.34 (d, 15.0)
3	6.96 (d, 15.0)	7.38 (d, 15.0)	6.95 (d, 15.0)	7.38 (d, 15.0)	6.96 (d, 15.0)	7.39 (d, 15.0)
-SCH ₃	2.94 (s)	3.09 (s)	2.94 (s)	3.09 (s)	2.94 (s)	3.09 (s)
-NCH ₃	3.06 (s)	3.05 (s)	3.06 (s)	3.07 (s)	3.06 (s)	3.06 (s)
1'	3.68 (t, 6.3)	3.63 (t, 7.5)	3.69 (t, 6.3)	3.64 (t, 7.5)	3.68 (t, 6.3)	3.63 (t, 7.2)
2'	2.84 (t, 6.3)	2.82 (t, 7.5)	2.85 (t, 6.3)	2.83 (t, 7.5)	2.84 (t, 6.3)	2.82 (t, 7.2)
4', 8'	7.04 (d, 8.4)	7.15 (d, 8.4)	7.06 (d, 8.4)	7.17 (d, 8.4)	7.04 (d, 8.4)	7.15 (d, 8.4)
5', 7'	6.87 (d, 8.4)	6.90 (d, 8.4)	6.84 (d, 8.4)	6.86 (d, 8.4)	6.83 (d, 8.4)	6.85 (d, 8.4)
1''	4.21 (m)	4.21 (m)	4.26 (dd, 3.6, 9.6); 4.02 (dd, 4.8, 9.6)	4.26 (dd, 3.6, 9.6); 4.02 (dd, 4.8, 9.6)	4.53 (d, 6.6)	4.53 (d, 6.6)
2''	2.20 (m)	2.20 (m)	2.15 (br s)	2.15 (br s)	5.46 (t, 6.6)	5.46 (t, 6.6)
4''	1.78 (m); 1.51 (m)	1.78 (m); 1.51 (m)	5.39 (br s)	5.39 (br s)	2.10 (t, 7.8)	2.10 (t, 7.8)
5''	1.69 (m); 1.16 (m)	1.69 (m); 1.16 (m)	2.26 (m) / 2.05 (m)	2.26 (m) / 2.05 (m)	1.72 (m)	1.72 (m)
6''			3.43 (dd, 5.4, 7.2)	3.43 (dd, 5.4, 7.2)	4.34 (m)	4.34 (m)
7''	3.60 (m)	3.60 (m)				
8''	0.97 (s)	0.97 (s)	1.06 (s)	1.07 (s)		
9''	1.00 (s)	1.00 (s)	0.94 (s)	0.95 (s)		
10''	1.24 (s)	1.24 (s)	1.73 (s)	1.73 (s)	1.75 (s)	1.75 (s)
6''-OMe					3.30 (s)	3.30 (s)
6''-OMe					3.30 (s)	3.30 (s)

^a Left column *s-cis*, right column *s-trans*.

Table 2 ^1H Spectroscopic Data for Compounds 4–6 in CD_3OD .

No.	4 ^a	4 ^a	5 ^a	5 ^a	6
2	6.78 (d, 15.0)	7.34 (d, 15.0)	2.47 (t, 7.2)	2.86 (t, 7.2)	4.83 (dd, 2.7, 10.5)
3	6.96 (d, 15.0)	7.39 (d, 15.0)	3.14 (t, 7.2)	3.39 (t, 7.2)	4.04 (dd, 10.2, 15.0) / 3.41 (d, 15.6)
-SCH ₃	2.92 (s)	3.09 (s)	2.95 (s)	2.96 (s)	2.92 (s)
-NCH ₃	3.08 (s)	3.07 (s)	2.86 (s)	2.98 (s)	3.03 (s)
1'	3.71(t, 6.0)	3.66 (t, 7.5)	3.59 (t, 6.6)	3.56 (t, 7.5)	3.70 (dd, 9.0, 12.6); 3.51 (dd, 3.0, 12.6)
2'	2.84 (t, 6.0)	2.82 (t, 7.5)	2.84 (t, 6.6)	2.76 (t, 7.5)	5.12 (dd, 3.3, 9.3)
4'	6.76(d, 1.8)	6.88(d,1.8)	7.12 (d, 8.4)	7.13 (d, 7.8)	7.37 (d, 8.4)
5'			6.84 (d, 8.4)	6.86 (d, 8.4)	6.93 (d, 8.4)
7'	6.83(d, 7.8)	6.86 (d, 7.8)	6.84 (d, 8.4)	6.86 (d, 8.4)	6.93 (d, 8.4)
8'	6.59 (dd, 8.4,1.8)	6.76 (dd, 8.4,1.8)	7.12 (d, 8.4)	7.17 (d, 7.8)	7.37 (d, 8.4)
1''	4.55 (d, 6.0)	4.55 (d, 6.0)	4.54 (d, 6.0)	4.52 (d, 6.0)	4.56 (d, 6.6)
2''	5.45(t, 6.6)	5.45(t, 6.6)	5.47 (t, 6.3)	5.47 (t, 6.3)	5.44 (t, 6.0)
4''	2.06 (t, 7.5)	2.06 (t, 7.5)	2.12 (m); 2.05 (m)	2.12 (m); 2.05 (m)	2.07 (t, 7.2)
5''	2.13(q, 6.6)	2.13(q, 6.6)	1.65 (m)	1.65 (m)	2.13 (q, 7.2)
6''	5.10(t, 6.6)	5.10(t, 6.6)	3.98 (t, 6.6)	3.98 (t, 6.6)	5.09 (m)
8''	1.61(s)	1.61(s)	4.81 (br s); 4.91 (br s)	4.81 (br s); 4.91 (br s)	1.66 (s)
9''	1.66(s)	1.66(s)	1.71 (s)	1.71 (s)	1.60 (s)
10''	1.72 (s)	1.72 (s)	1.75 (s)	1.75 (s)	1.74 (s)
5'-OMe	3.83(s)	3.83(s)			

^a Left column *s-cis*, right column *s-trans*.**Table 3** ^{13}C Spectroscopic Data for Compounds 1–6 in CD_3OD .

No.	1 ^a	1 ^a	2 ^a	2 ^a	3 ^a	3 ^a	4 ^a	4 ^a	5 ^a	5 ^a	6
1	165.6	165.1	165.6	165.2	165.6	165.1	165.6	165.1	171.7	171.5	168.2
2	133.3	134.4	133.7	134.5	133.3	134.4	133.0	134.4	27.0	27.8	73.3
3	139.8	140.9	139.8	140.9	139.9	140.9	139.9	140.9	51.4	51.3	56.3
-SCH ₃	42.6	42.4	42.6	42.4	42.5	42.4	42.5	42.4	41.0	41.3	43.1
-NCH ₃	34.6	36.9	34.5	36.9	34.6	36.9	34.6	36.7	34.3	36.5	35.1
1'	53.4	51.7	53.4	51.7	53.4	51.7	53.3	51.6	53.0	51.6	55.0
2'	34.5	33.4	34.5	33.4	34.5	33.4	34.8	33.9	34.4	33.7	71.8
3'	131.1	131.9	131.5	132.3	131.3	132.1	132.3	132.3	131.2	132.4	130.4
4'	131.6	131.0	131.6	131.1	131.5	131.0	114.2	114.1	131.3	131.0	129.2
5'	116.2	115.9	116.2	115.9	116.3	116.1	151.3	151.3	116.3	116.0	116.1
6'	160.0	159.7	159.3	159.0	159.5	159.1	148.3	148.3	159.4	159.0	160.7
7'	116.2	115.9	116.2	115.9	116.3	116.1	115.5	115.8	116.3	116.0	116.1
8'	131.6	131.0	131.6	131.1	131.5	131.0	122.9	122.3	131.3	131.0	129.2
1''	66.2	66.2	68.4	68.3	65.9	65.9	67.1	67.2	65.9	66.0	66.0
2''	47.9	47.8	50.8	50.8	121.6	121.7	121.3	121.4	121.5	121.6	121.3
3''	72.9	72.9	135.2	135.2	141.4	141.4	142.1	142.1	141.9	141.7	142.1
4''	39.4	39.4	121.4	121.4	35.5	35.5	40.8	40.8	36.7	36.7	40.8
5''	32.7	32.7	32.7	32.7	32.0	32.0	27.5	27.5	34.2	34.2	27.5
6''	35.6	35.6	74.9	74.9	105.9	105.9	125.2	125.2	76.2	76.2	125.1
7''	75.2	75.2	38.4	38.4			132.7	132.7	148.9	148.9	132.7
8''	28.6	28.6	26.9	26.9			17.9	17.9	111.7	111.7	26.1
9''	25.2	25.2	18.6	18.7			26.1	26.1	17.8	17.8	17.9
10''	24.4	24.4	22.8	22.7	16.8	16.8	16.8	16.8	16.8	16.8	16.8
5'-OMe							56.4	56.6			
6''-OMe					53.6	53.6					
6''-OMe					53.6	53.6					

^a Left column *s-cis*, right column *s-trans*.

formers a and b in 2.5:1. In addition to the characteristic signals of (*E*)-3-(methylsulfonyl)propenoic acid moiety and *N*-methyltyramine part, compound **1** also contained 10 carbon signals, including three methyls [δ_{C} 28.6 (q), 25.2 (q), 24.4 (q)], two methylenes [δ_{C} 39.4 (t), 32.7 (t)], one oxygenated methylene [δ_{C} 66.2 (t)], one methine [δ_{C} 47.9 (d)], one oxy-

genated methine [δ_{C} 75.2 (d)], one sp^3 quaternary carbon [δ_{C} 35.6 (s)], and one oxygenated sp^3 tertiary carbon [δ_{C} 72.9 (s)]. Careful analysis of the 2D NMR (Fig. S4-S6, SI) yielded two structural fragments (A) $-\text{CH}_2(4'')\text{CH}_2(5'')$ - and (B) $-\text{CH}_2(1'')(\text{O})\text{CH}(2'')\text{CH}(7'')(\text{O})-$. HMBC correlations (Fig. 2) from CH_3-10'' [δ_{H} 1.24 (s)] to δ_{C} 72.9 (s, C-3''), 39.4 (t, C-

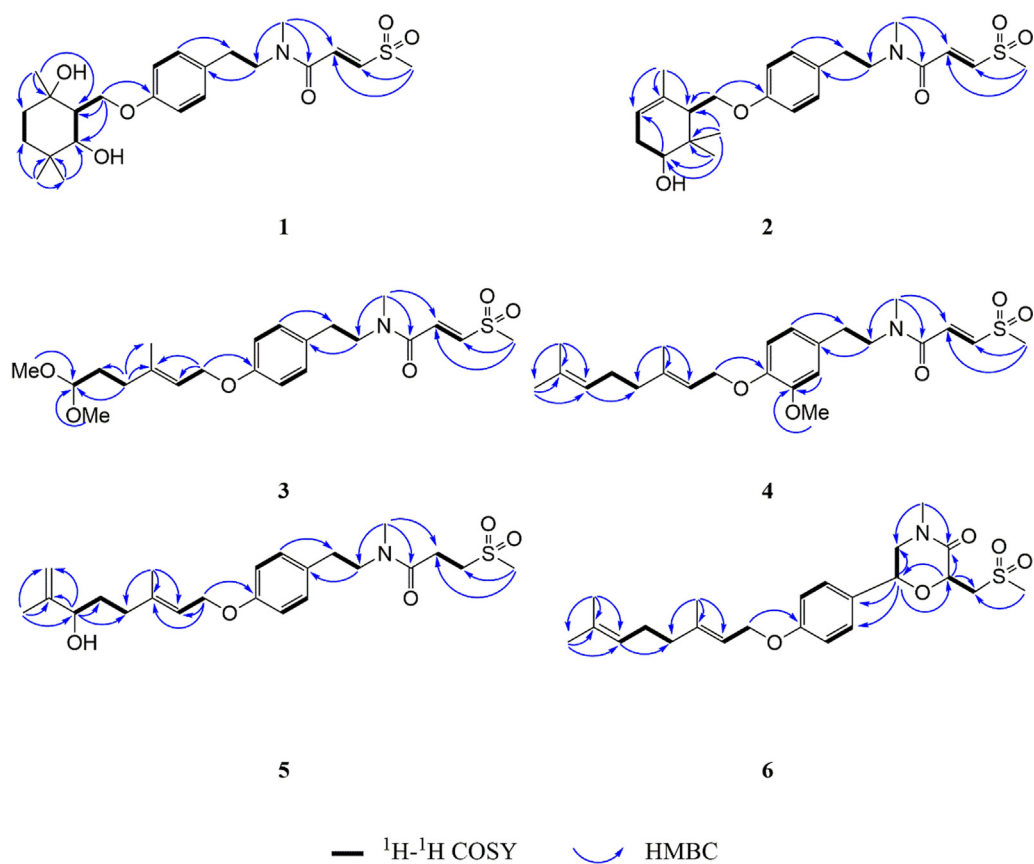


Fig. 2 Key HMBC and ^1H - ^1H COSY correlations of compounds 1–6.

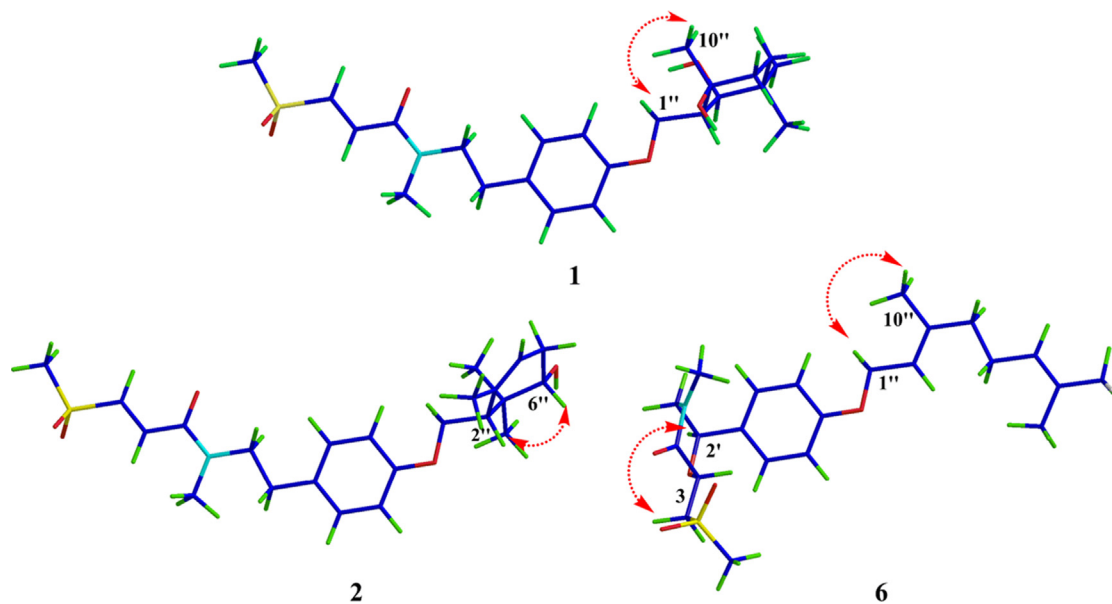


Fig. 3 ROESY correlations for compounds 1, 2 and 6.

4''), and 47.9 (d, C-2''), and from CH_3 -8'' [δ_{H} 0.97 (s)] and CH_3 -9'' [δ_{H} 1.00 (s)] to δ_{C} 75.2 (d, C-7''), 35.6 (s, C-6''), and 32.7 (t, C-5'') suggested that two structural fragments A and B were connected to C-3'' through C-4'' and C-2'', and C-6'' through C-5'' and C-7'' respectively. Therefore, the remaining

carbon signals could establish 2-oxymethylene-1, 4, 4-trimethylcyclohexane-1, 3-diol moiety. Moreover, HMBC correlations from CH_2 -1'' [δ_{H} 4.21] to δ_{C} 160.0 (s, C-6') implied that this moiety was connected to C-6'. In ROESY spectrum (Fig. S7, SI), the correlation of H_3 -10'' with H_2 -1'' implied that

3''-OH and H-2'' were co-facial. The relative configuration of C-7'' could not be determined due to the lack of useful ROESY correlations. Therefore, to further verify the relative configuration of C-7'', two isomers (2''S*, 3''S*, 7''R*)-**1a** and (2''S*, 3''S*, 7''S*)-**1b** were subjected to NMR calculations with the DP4 + analysis. These results showed that (2''S*, 3''S*, 7''R*)-**1a** (Figs. 4-5, Tables S3, S5, and S7-S8, Fig. 65, SI) was the most likely structure for **1** with a 100.00 % DP4 + probability based on all NMR data (Marcarino et al., 2020). This determined the relative configuration of **1**. Compound **1** has a small optical rotation value and no cotton effect in the CD spectrum, indicating that they may be a racemic mixture, which was further resolved by chiral column [column: CHIRALPAK® IC 4.6 × 250 mm 5 μm; mobile phase: MeCN: H₂O (30:70); flow rate: 0.5 ml/min; detection: UV, 225 nm] to give a pair of enantiomer **1a** and **1a'** at *t_R* 54.3 and 46.9 min respectively. By comparing the experimental ECD data with the calculated results, the absolute configurations of **1a/1a'** were assigned as (2''S, 3''S, 7''R)-**1a** and (2''R, 3''R, 7''S)-**1a'** (Fig. 6). Therefore, the structure of **1** was determined as shown in Fig. 1, and denoted as glycopentamide S.

The molecular formula of **2** was deduced to be C₂₃H₃₃NO₅S through HR-ESI-MS (Fig.S21, SI) at *m/z* 458.19687 [M + Na]⁺ (calcd for C₂₃H₃₃NO₅SNa, 458.19716), which was composed of two conformers a and b in 2.3:1. Careful comparison of the NMR data of compounds **1** and **2** revealed that compound **2** was the absence of one oxygenated tertiary carbon and methylene, but had one more tri-substituted double bond. It was speculated that compound **2** might be the dehydration product of **1**. However, through careful analysis of the 2D NMR (Fig. S17-S18, SI), two structural fragments (A) -CH(4'')CH₂(5'')CH(6'')(O)- and (B) -CH₂(1'')(O)CH(2'')- were obtained which were completely different from the dehydration product of **1**. In the same way, HMBC correlations from CH₃-10'' [δ_H 1.73 (s)] to δ_C 135.2 (s, C-3''), 121.4 (d, C-4''), and 50.8 (d, C-2''), and from CH₃-8'' [δ_H 1.06 (s)] and CH₃-9'' [δ_H 0.94 (s)] to δ_C 74.9 (d, C-6''), 38.4 (s, C-7''), and 50.8 (d, C-2'') constructed 5-oxymethylene-4,6,6-trimethyl cyclohex-3-en-1-ol moiety, which was connected to C-6' by HMBC correlation from CH₂-1'' [δ_H 4.26, 4.02] to δ_C 159.3 (s, C-6'). The relative configuration of **2** was determined by interpreting the ROESY spectrum (Fig. 3, Fig. S19, SI), where the correlation of H-2'' with H-6'' indicated that these protons

were co-facial. NMR calculations further confirmed the relative configuration of **2** (Tables S4 and S6, SI). At the B3LYP/6-31 + G(d) level, the absolute configuration of **2** was determined by the ECD calculations using the TDDFT/ECD method. The calculated ECD curve of (2''S, 6''R)-**2** was in good agreement with the experimental ECD spectrum (Fig. 6). Therefore, the absolute configuration of **2** was shown in Fig. 1, and denoted as glycopentamide T.

The molecular formula of **3** was deduced to be C₂₂H₃₃NO₆S through HR-ESI-MS (Fig. S31, SI) at *m/z* 462.19199 [M + Na]⁺ (calcd for C₂₂H₃₃NO₆SNa, 462.19208), which was composed of two conformers a and b in 2.6:1. Its ¹H and ¹³C NMR data (Fig. 23-25, SI) were similar to those of methylambullin (Greger et al., 1994), except for the presence of a 1,1-dimethoxyethyl group at C-4'' [δ_H 1.72 (2H, m), 4.34 (1H, m), 3.30 (6H, s); δ_C 32.0 (t), 105.9 (d), 2 × 53.6 (q)] in **3** instead of a prenyl group at C-4'' in methylambullin. Thus, compound **3** was the oxidation product of the double bond Δ^{6''} (7'') of methylambullin, resulting in the loss of three carbon atoms. These result was further supported by HMBC correlations (Fig. 27, SI) from CH₃O- [δ_H 3.30(s)] to δ_C 105.9 (d, C-6'') and from H₂-4'' [δ_H 2.10] to δ_C 105.9 (d, C-6''), and ¹H-¹H COSY of -CH(6'')CH₂(5'')CH₂(4'')-. Moreover, the configuration of double bond Δ^{2''}(3'') was assigned as *E* based on ROESY correlation of Me-10''/H₂-1''. Thus, the structure of **3** was determined as shown in Fig. 1, and denoted as glycopentamide U.

The molecular formula of **4** was deduced to be C₂₄H₃₅NO₅S through HR-ESI-MS (Fig. S40, SI) at *m/z* 450.23120 [M + H]⁺ (calcd for C₂₄H₃₆NO₅S, 450.23087), which was composed of two conformers a and b in 2.6:1. By comparing with the NMR data (Fig. S32-34, SI) of methylambullin and methylgerambullin, it was found that the substituent pattern of **4** on the benzene ring was different from that of methylambullin and methylgerambullin (Greger et al., 1994). The *para*-substitution pattern of the benzene ring of methylambullin and methylgerambullin was replaced by the 1,2,4-trisubstitution benzene ring of **4**. HMBC correlations (Fig. S36, SI) from H-4' [δ_H 6.76] and MeO [δ_H 3.83] to δ_C 151.3 (s, C-5'), from H-1'' [δ_H 4.55] to δ_C 148.3 (s, C-6'), and ROESY correlations (Fig. S38, SI) from MeO to H-4' confirmed the methoxyl and geranyloxy were attached to C-5' and C-6', respectively. Moreover, the configuration of double

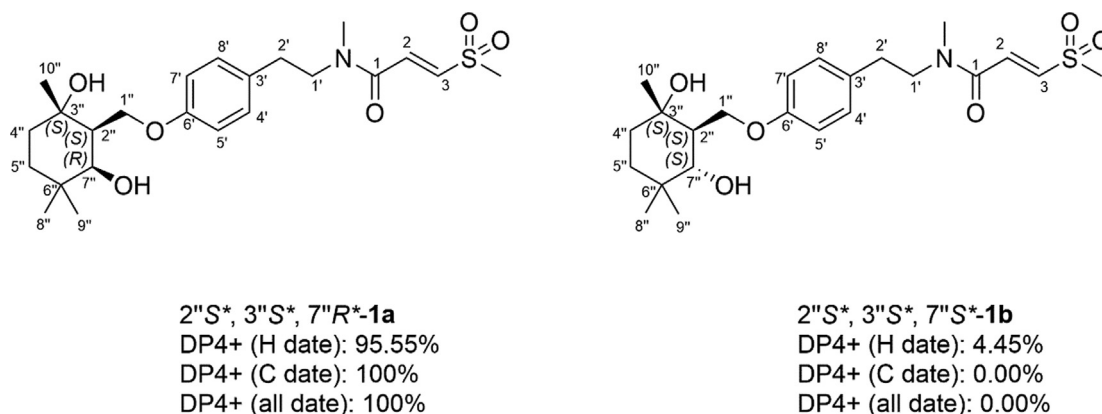


Fig. 4 DP4 + analysis of two possible diastereomers (**1a** and **1b**) for **1**.

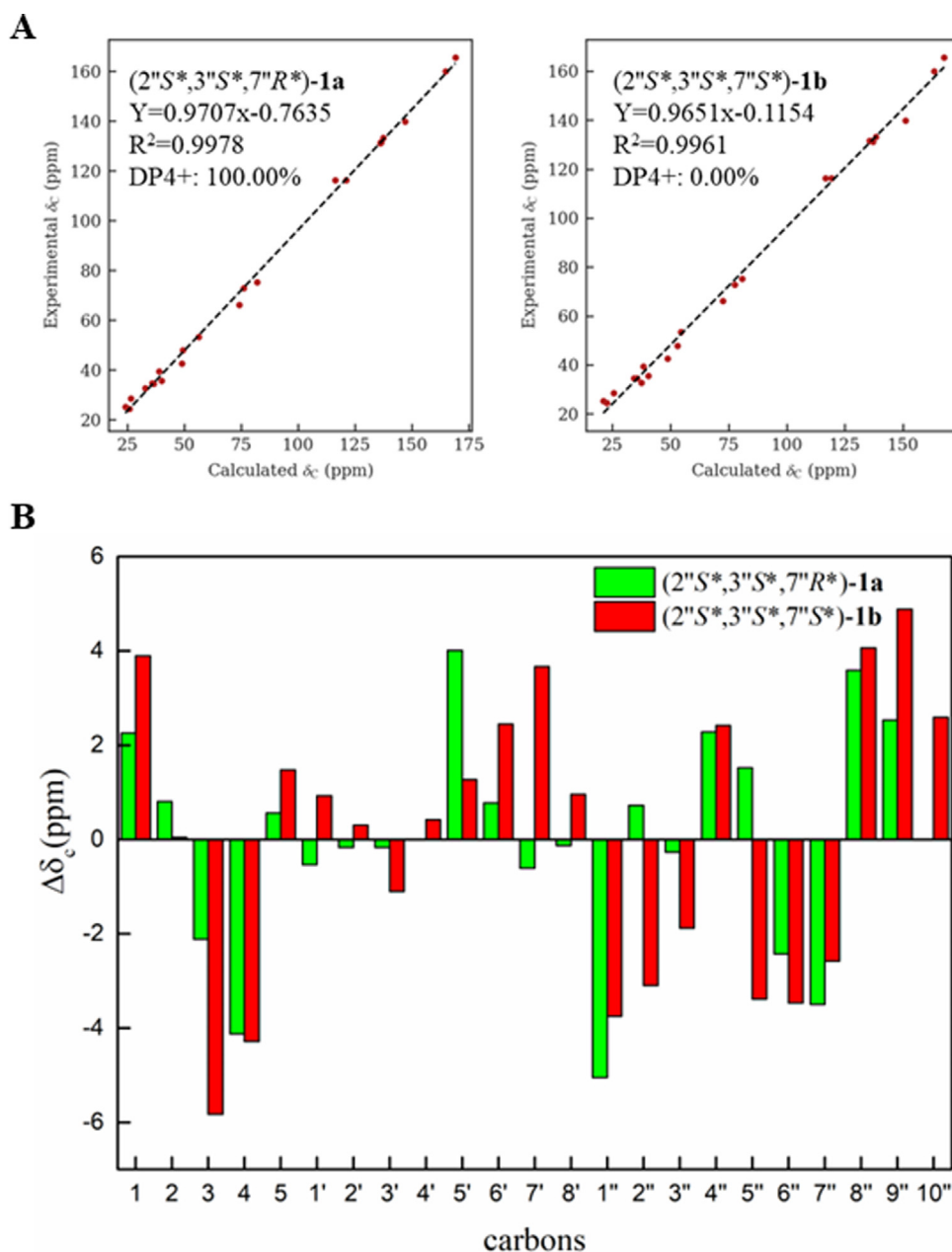


Fig. 5 (A) Linear regression fitting of calculated ^{13}C chemical shifts of two possible isomers of **1a** and **1b** with the experimental values (B) Deviation between calculated ^{13}C chemical shifts of two possible isomers of **1a** and **1b** with the experimental values.

bond $\Delta^{2''(3'')}$ was established as *E* through ROESY correlation of Me-10'' with H₂-1''. Thus, the structure of **4** was determined as shown in Fig. 1, and denoted as glycopentamide V.

The molecular formula of **5** was deduced to be C₂₃H₃₅NO₅-S through HR-ESI-MS (Fig. S48, SI) at *m/z* 460.21243 [M + Na]⁺ (calcd for C₂₃H₃₅NO₅SNa, 460.21282), which was composed of two conformers a and b in 1:1. The NMR data of compound **5** (Fig. S41-43, SI) were similar to those of glycopentamide B (Nian et al., 2020), except that glycopentamide B had a *trans* double bond $\Delta^{1(2)}$ [δ_{H} 6.80 (d, *J* = 15.0 Hz), δ_{C} 133.3; δ_{H} 6.95 (d, *J* = 15.0 Hz), δ_{C} 139.8], while **5** had two methylene signals [δ_{H} 3.14 (t, *J* = 7.2 Hz), δ_{C} 51.4; δ_{H} 2.47 (t, *J* = 7.2 Hz), δ_{C} 27.0], indicating that **5** was the saturated product of the double bond $\Delta^{1(2)}$ of gly-

copentamide B. This deduction was further confirmed by HMBC correlations (Fig. S45, SI) from H₂-2 [δ_{H} 2.47] and H₂-3 [δ_{H} 3.14] to δ_{C} 171.7 (s, C-1), and ¹H-¹H COSY of -CH₂(2)CH₂(3)-. The absolute configuration of **5** was assigned as 6'*S* based on the ECD calculations. Thus, the structure of **5** was determined as shown in Fig. 1, and denoted as glycopentamide W.

The molecular formula of **6** was deduced to be C₂₃H₃₃NO₅-S through HR-ESI-MS (Fig. S58, SI) at *m/z* 458.19693 [M + Na]⁺ (calcd for C₂₃H₃₃NO₅SNa, 458.19716). Interestingly, a comparison of the NMR data of **1-5** with that of **6** (Fig. S50-52, SI) showed that **6** displayed only one set of NMR signals, indicating that **6** lacked the *s-cis* and *s-trans* conformers. A comparison of its NMR data with those of

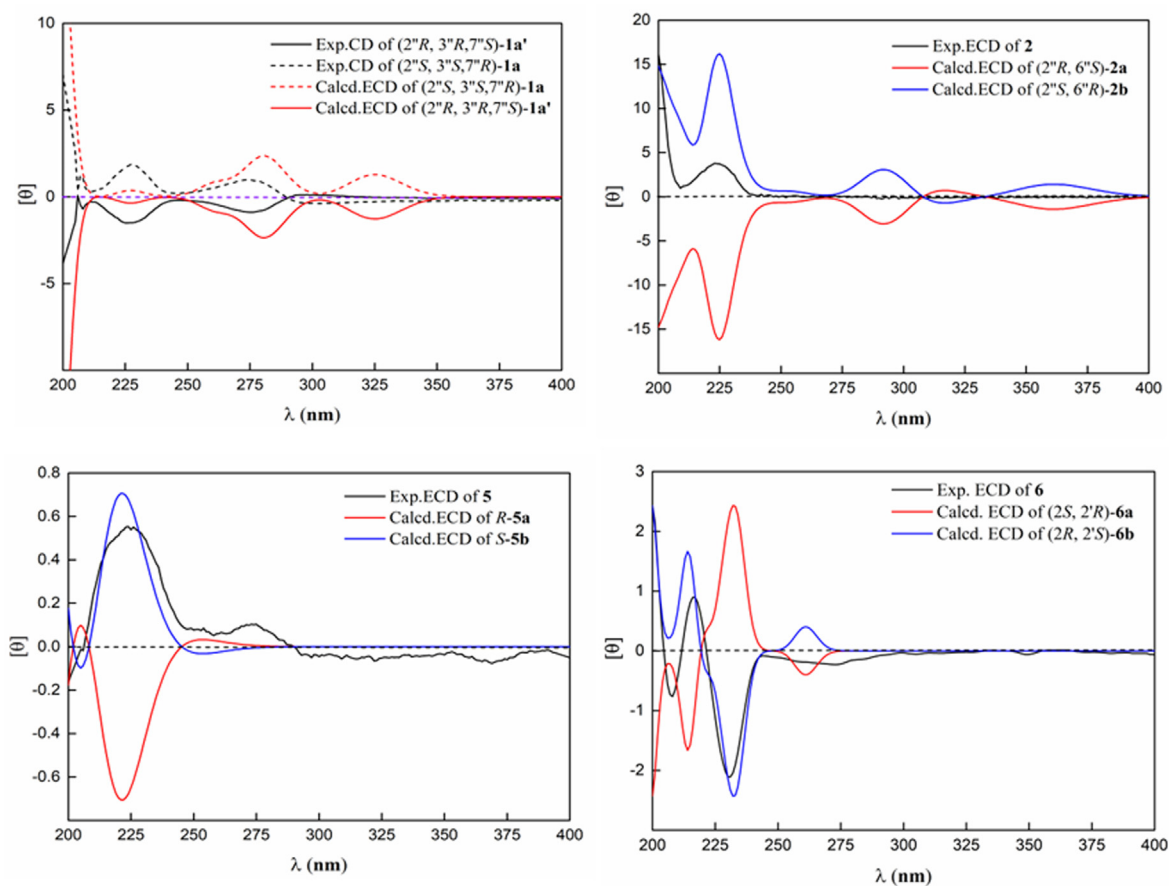


Fig. 6 Calculated and experimental ECD spectra of **1**, **2**, **5** and **6**.

methylumbelliferone and methylgerambullin implied that they possessed *para*-geranyloxy phenyl group (Greger et al., 1994). Apart from the abovementioned signals, the remaining signals included two methyls [δ_C 43.1 (q), 35.1(q)], two oxygenated methines [δ_C 73.3 (d); 71.8 (d)], two methylenes [δ_C 55.0 (t); 56.3 (t)], and one carbonyl [δ_C 168.2 (s)]. Detailed analysis of ^{13}C NMR data of compounds **1–6** suggested that the two methyls were connected to *N* atom and sulfonyl respectively. Two structural fragments (A) $-\text{CH}_2(1')\text{CH}(2')$ (O)- and (B) $-\text{CH}_2(3)\text{CH}(2)\text{O}$ - were obtained by careful analysis of the 2D NMR (Fig. S53-55, SI). HMBC correlations from $-\text{NCH}_3$ [δ_H 3.03 (s)] to δ_C 55.0 (t, C-1') and 168.2 (s, C-1), and from H-2 [δ_H 4.83] to δ_C 71.8 (d, C-2'), 168.2 (s, C-1) and 56.3 (t, C-3) suggested that two structural fragments A and B were connected to *N* through C-1' and C-1, and connected by ether bond through C-2 to C-2'. Therefore, 4-methyl-2-((methylsulfonyl)methyl) morpholin-3-one moiety could be established. HMBC correlations from H-2' [δ_H 5.12] to δ_C 129.2 (d, C-4', 8') confirmed the morpholin-3-one moiety was connected to C-3'. The relative configuration of **6** was determined by interpreting the ROESY spectrum (Fig. S56, SI), where the correlation of H-2' with H₂-3 indicated that these protons were co-facial and H-2' and H-2 were assigned *trans*. The absolute configuration of **6** was determined by comparing the experimental and calculated ECD spectra. Consequently, the absolute configuration of **6** was defined as (2*R*, 2'*S*)-**6**. Therefore, the absolute configuration of **6** was shown in Fig. 1, and denoted as glycopentamide X.

The inhibitory effect of these compounds on HepG2 cell proliferation was determined by CCK-8 method, and their anti-inflammatory effects were assessed by inhibiting the activity of NO production stimulated by lipopolysaccharide in mouse macrophage RAW 264.7 cells (Table S9). As a result, only compound **4** significantly inhibited lipopolysaccharide-induced NO production in mouse macrophage RAW 264.7 cells with the IC_{50} value of 0.55 μM (dexamethasone as a positive control, IC_{50} : 9.24 μM). The remaining compounds were inactive showing IC_{50} values in excess of 20 μM . Moreover, compounds **3** and **4** exhibited different anti-proliferative activities against HepG-2 with IC_{50} values of 11.52 and 9.41 μM , respectively (cisplatin as a positive control, IC_{50} : 5.96 μM). The other compounds showed no obviously anti-proliferative activities with IC_{50} values in excess of 20 μM . Based on previous research and our results (Nian et al., 2020), the geranyloxy group at C-6' of these methylsulfonylpropenoic acid amides might be crucial for the anti-proliferative and anti-inflammatory activities.

4. Conclusions

Sulfur-containing amides are a special type of alkaloids, and mainly isolated from the genus *Glycosmis*. This compounds showed novel structure and exhibited diversity bioactivity, like antimicrobial, cytotoxic, antitrypanosomal, antiviral activities. In this paper, six previously undescribed sulfur-containing amides with structural diversities were isolated from the leaves of *G. pentaphylla*. It is noteworthy that

6 represents the first example of sulfur-containing amide possessing a morpholin-3-one moiety. Moreover, Compound 4 had the strongest proliferative activity on HepG2 cells and had a significant inhibitory effect on NO production. The relationship between structure and activity indicates that the geranyloxy group at C-6' plays an important role in the anti-inflammatory and anti-proliferative activities of these alkaloids. These findings indicate that among the active ingredients of *G. pentaphylla* that exert anti-inflammatory and anticancer activities, in addition to the flavonoids reported in the previous literature (Shoja et al., 2015; Shoja et al., 2016), sulfur-containing amides also play an important role. These findings could explain the traditional use of *G. pentaphylla* to treat liver cancer and inflammatory diseases and provide a scientific basis for traditional medicine knowledge.

CRedit authorship contribution statement

Wenli Xie: Investigation, Formal analysis, Writing – original draft. **Hefeng Nian:** Investigation, Formal analysis. **Xueni Li:** Formal analysis. **Jing Xu:** Formal analysis. **Yu Chen:** Formal analysis. **Zhinan Mei:** Supervision, Writing – review & editing. **Guangzhong Yang:** Supervision, Writing – review & editing.

Declaration of Competing Interest

The authors declare that they have no known competing financial interests or personal relationships that could have appeared to influence the work reported in this paper.

Acknowledgements

This work was supported by the National Key Research and Development Program (2022YFC3502200), the Key Research and Development Program of Hubei Province (2021ACB003), and the Major Scientific and Technological Project of Hubei Province (2020ACA007).

Appendix A. Supplementary material

Supplementary data to this article can be found online at <https://doi.org/10.1016/j.arabjc.2022.104528>.

References

- Chen, Y., Ma, Z., Teng, H., Gan, F., Xiong, H., Mei, Z., Yang, G., 2019. Adamantyl and homoadamantyl derivatives from *Garcinia multiflora* fruits. *RSC Adv.* 9, 12291–12299.
- Greger, H., Hofer, O., Zechner, G., Hadacek, F., Wurz, G., 1994. Sulphones derived from methylthiopropenoic acid amides from *Glycosmis angustifolia*. *Phytochemistry* 37, 1305–1310.
- Hofer, O., & Greger, H. 2000. Sulfur-containing amides from *Glycosmis* species (Rutaceae). in: Herz W., Falk H., Kirby G.W., Moore R. E. (Eds.), *Prog. Chem. Org. Nat. Prod.*, 187–223.
- Hofer, O., Zechner, G., Vajrodaya, S., Lutz, G., Greger, H., 1995. New anthranilic and methylsulfonylpropenoic acid amides from Thai *Glycosmis* species. *Liebigs Ann* 1995, 1789–1794.
- Hofer, O., Vajrodaya, S., Greger, H., 1998. Phenethylamides with an unusual 4-oxo-2-oxolenyl terpenoid side chain from *Glycosmis* species. *Monatsh. Chem.* 129, 213–219.
- Hofer, O., Greger, H., Lukaseder, B., Vajrodaya, S., Bacher, M., 2000. Prenylated sulfonyl amides from *Glycosmis* species. *Phytochemistry* 54, 207–213.
- Khandokar, L., Bari, M.S., Seidel, V., Haque, M.A., 2021. Ethnomedicinal uses, phytochemistry, pharmacological activities and toxicological profile of *Glycosmis pentaphylla* (Retz.) DC.: A review. *J. Ethnopharmacol.* 278, 114313.
- Marcarino, M.O., Zanardi, M.M., Cicetti, S., Sarotti, A.M., 2020. NMR calculations with quantum methods: development of new tools for structural elucidation and beyond. *Acc. Chem. Res.* 53, 1922–1932.
- Moon, J.T., Ha, S.H., Lee, S.H., Kwon, T.H., Oh, C.R., Kim, Y.D., Lee, J.Y., 2010. Total synthesis and biological evaluation of methylgerambullone. *Bioorg. Med. Chem. Lett.* 20, 52–55.
- Nian, H., Xiong, H., Zhong, F., Teng, H., Teng, H., Chen, Y., Yang, G., 2020. Anti-inflammatory and antiproliferative prenylated sulphur-containing amides from the leaves of *Glycosmis pentaphylla*. *Fitoterapia* 146, 104693.
- Shoja, M.H., Reddy, N.D., Nayak, P.G., Srinivasan, K.K., Rao, C. M., 2015. *Glycosmis pentaphylla* (Retz.) DC arrests cell cycle and induces apoptosis via caspase-3/7 activation in breast cancer cells. *J. Ethnopharmacol.* 168, 50–60.
- Shoja, M.H., Reddy, N.D., Nayak, P.G., Biswas, S., Srinivasan, K.K., Rao, C.M., 2016. In vitro mechanistic and in vivo anti-tumor studies of *Glycosmis pentaphylla* (Retz.) DC against breast cancer. *J. Ethnopharmacol.* 186, 159–168.
- Sutton, P., Newcombe, N.R., Waring, P., Müllbacher, A., 1994. In vivo immunosuppressive activity of gliotoxin, a metabolite produced by human pathogenic fungi. *Infect. Immun.* 62, 1192–1198.
- Teng, H., Ren, Y., Ma, Z., Tan, X., Xu, J., Chen, Y., Yang, G., 2019. Homoadamantane polycyclic polyprenylated acylphloroglucinols from the fruits of *Garcinia multiflora*. *Fitoterapia* 137, 104245.
- Vajrodaya, S., Bacher, M., Greger, H., Hofer, O., 1998. Organ-specific chemical differences in *Glycosmis trichanthera*. *Phytochemistry* 48, 897–902.
- Wu, C., Shu, G., Huang, H., Pang, K., Yang, X., Yang, G., 2021. Methylgerambullin derived from plant *Glycosmis pentaphylla* (Retz.) correa. Mediates anti-hepatocellular carcinoma cancer effect by activating mitochondrial and endoplasmic reticulum stress signaling and inhibiting AKT and STAT3 pathways. *Food Chem. Toxicol.* 149, 112031.
- Yang, K., Guo, S.S., Geng, Z.F., You, C.X., Zhang, W.J., Li, Y.P., Deng, Z.W., 2015. Five new sulphur-containing amides from *Glycosmis lucida* with antifeedant activity against *Tribolium castaneum*. *Ind. Crop. Prod.* 74, 628–634.
- Yasir, M., Tripathi, M.K., Singh, P., Shrivastava, R., 2019. The genus *Glycosmis* [Rutaceae]: a comprehensive review on its phytochemical and pharmacological perspectives. *The Nat. Prod. J.* 9 (2), 98–124.